Carbohydrate Polymers 102 (2014) 986–992

Contents lists available at ScienceDirect

Carbohydrate Polymers

journal homepage: www.elsevier.com/locate/carbpol

Synthesis and electrospinning carboxymethyl cellulose lithium (CMC-Li) modified 9,10-anthraquinone (AQ) high-rate lithium-ion battery

Lei Qiu[a,b], Ziqiang Shao[a,b,*], Minglong Liu[c], Jianquan Wang[a,b], Pengfa Li[c], Ming Zhao[d]

[a] College of Material Science and Engineering, Beijing Institute of Technology, Beijing 100081, PR China
[b] Beijing Engineering Technology Research Center for Cellulose and Its Derivative Materials, Beijing 100081, PR China
[c] School of Chemical Engineering and Environment, Beijing Institute of Technology, Beijing 100081, PR China
[d] North Century Cellulose Technology Research & Development Co., Ltd., Beijing 100081, PR China

ARTICLE INFO

Article history:
Received 29 July 2013
Received in revised form
16 September 2013
Accepted 19 September 2013
Available online 29 October 2013

Keywords:
Electrospinning
Cellulose derivatives
Lithium-ion battery
Anode materials AQ
CMC-Li

ABSTRACT

New cellulose derivative CMC-Li was synthesized, and nanometer CMC-Li fiber was applied to lithium-ion battery and coated with AQ by electrospinning. Under the protection of inert gas, modified AQ/carbon nanofibers (CNF)/Li nanometer composite material was obtained by carbonization in 280 °C as lithium battery anode materials for the first time. The morphologies and structures performance of materials were characterized by using IR, ^{1}H NMR, SEM, CV and EIS, respectively. Specific capacity was increased from 197 to 226.4 mAh g^{-1} after modification for the first discharge at the rate of 2C. Irreversible reduction reaction peaks of modified material appeared between 1.5 and 1.7 V and the lowest oxidation reduction peak of the difference were 0.42 V, the polarization was weaker. Performance of cell with CMC-Li with the high degree of substitution (DS) was superior to that with low DS. Cellulose materials were applied to lithium battery to improve battery performance by electrospinning.

1. Introduction

In today's energy society, lithium-ion batteries become energy of many portable electronic devices due to their superior voltage, high-energy density, low environmental pollution (Lee et al., 2006). The raw materials (Chaudhari et al., 2013) of anode material of organics derived from nature has the properties of excellent capacity, abundant material, friendly environment, which attracts more attention. In such materials, conjugated conductive polymer (Abouimrane et al., 2013) is a kind of widely studied material, the performance of poly aniline is the best among them. Oyama, Pope, and Sotomura (1997) proposed implementation of electrochemistry by doping anionic, but the energy density of the battery was low. Another representative organic cathode material was sulfide based on S—S bond breaking and bonding to charge and discharge. However, it led to the poor loop stability due to the difficulty of dissolution. Carbonyl compounds represented by AQ and its polymer (Wang et al., 2012; Xie et al., 2012), and anhydrides with conjugated structure are widely concerned as a new kind of anode material. Their electrochemical reaction mechanism (Teh, Sharma, Pramana, & Srinivasan, 2011) is that the oxygen atom in each carbonyl gets an electron when charging, and the electron reacts with inserted lithium ion to obtain enol lithium. Lithium ion is prolapsed when discharging and carbonyl are restored. The conversion accomplishes the reversible insertion and prolapse of lithium ions, since AQ has good crystal structure, so it has excellent cycle performance. It is still hotspot and focus on the current study of active substance materials to be nano-crystallized (Wu et al., 2013), ion doped (Rousselot et al., 2012), carbon coated (Jian et al., 2012) and (Saji, Kim, Kim, Cho, & Song, 2011) composited with other materials. It enhances the conductivity, tap density, ratio and stability to satisfy high-rate charge or discharge of the battery. The application (Kong et al., 2013) of electrospinning provides a better way for the above research, while nanofiber material is obtained, and it also enhances performance of the battery by doping and carbon coating.

Cellulose materials have received wide attention of scholars in the research on electrospinning through a study on the different solvent systems. It focuses on cellulose ester and non-ionic cellulose ether, such as cellulose acetate (CA) (Rodriguez, Renneckar, & Gatenholm, 2011), Hydroxypropyl cellulose (HPC) (Chang & Zhang, 2011), Ethylcellulose (EC) (Yu et al., 2013), etc. Our laboratory also received many good results in cellulose, hydroxypropyl methyl cellulose (HPMC) (Ma et al., 2010), nitrocellulose (NC) (Xie, Shao,

* Corresponding author at: College of Material Science and Engineering, Beijing Institute of technology, Beijing 100081, PR China. Tel.: +86 10 68940942; fax: +86 10 68941797.
E-mail addresses: Shaoziqiang@263.net, qiulei1010@126.com (Z. Shao).

0144-8617/$ – see front matter © 2013 Elsevier Ltd. All rights reserved.
http://dx.doi.org/10.1016/j.carbpol.2013.09.105

Wang, & Wang, 2011) and its derivates, cellulose acetate butyrate (CAB) (Qiu et al., 2013) and its derivates, etc. The above materials are applied to lithium battery, explosives and powders, coating, capacitor, conductive paper (Gao et al., 2013). Ionic cellulose ether is a linear polyhydroxy cellulose derivative compound and has better rigid molecular structure (Karabulut, Pettersson, Ankerfors, & Wagberg, 2012), and it is as well an effective ion conductive polymer. It has merit (Canejo & Godinho, 2013) that the other materials can't compare with, such as low cost, easily soluble in water, environmentally friendly, simple technique. The suitable way of electrospinning has never been found due to the structure and property of ionic cellulose ether, so that there is no report on the study in the current time, especially the research on CMC-Li, which is blank in correlative research. It is thought to provide a diffusion pathway for lithium ions to reach the anode particle surface, increases the content of freely moving lithium ion in lithium-ion battery, and improves the prolapsing and embedding of lithium ion between anode and cathode electrode (Guerfi, Kaneko, Petitclerc, Mori, & Zaghib, 2007). To improve the charge and discharge capacity of the battery, it is also appropriate to be carbon-coated to obtain modified active materials, and it also has abundant lithium-ions of free ionization. We found the electrospinning method suitable for ionic cellulose ether and obtained nanometer CMC-Li fibers for the first time. The laboratory is currently conducting a study of functional materials, such as the application of electrospinning for coaxial (Hwang, Lee, Kong, Seo, & Choi, 2012), three axis (Zhou, Yin, Cao, Wan, & Guo, 2012), multilayer cross (Liu et al., 2013; Wang et al., 2013), etc. It is expected to make a breakthrough in nanocellulose product on membrane filtration materials (Lalia, Guillen-Burrieza, Arafat, & Hashaikeh, 2013), tissue engineering scaffold materials (Luo et al., 2013; Vulic & Shoichet, 2012), bioengineering (Luo et al., 2013), clinical medicine (Yu, Yu, Chen, Williams, & Wang, 2012), sensor (Ongun et al., 2013), lithium battery (Kraytsberg & Ein-Eli, 2012; Zhao et al., 2013) and supercapacitor (Zhang et al., 2013) through the above electrospinning method.

This study focuses on the development and synthesis of new ionic cellulose ether products CMC-Li with the different DS. CMC-Li, AQ/CMC-Li nanofiber are obtained by electrospinning for the first time, respectively. AQ/CNF/Li nanocomposite reactive material is obtained after carbonization under certain conditions, which enhance tap density, conductivity and the number of mobile lithium-ions. We also compare performance changes of batteries assembled by active substance before and after modification. Through the speculation and analysis of the model of battery mechanism, the paper compared the impact of different CMC-Li products on battery performance, which laid the foundation for CMC-Li in the application of battery material by electrospinning. It not only expands the type of electrospinning polymer, provides a polymer of easy operation and better performance for electrospinning, and fills the gap of the correlative research, but also supports a new research technique for the application of natural polysaccharides, especially the study on nanocrystallization of ionic cellulose ether material, which will certainly drive the research of the related material field, and it is significantly important.

2. Experimental

2.1. Materials

Purified cotton (M100) was supplied by Xi' An North Hui Chemical Industry Co., Ltd. (Xi' An, China). Methylene chloride (MC), monochloroacetic acid, glacial acetic acid, butyric acid, acetone, sulfuric acid (98% solution), ethanol (EtOH) was supplied by Beijing chemical fine chemical Co., Ltd. (Beijing, China). Polyethylene oxide (PEO), Lithium hydroxide monohydrate ($LiOH{\cdot}H_2O$), 9,10-Anthraquinone (AQ) were supplied by Alfa Aesar Chemical Co., Ltd. (Tianjin, China).

2.2. Synthesis of CMC-Li

The preparation process of CMC-Li can be clarified by the following schematic equation:

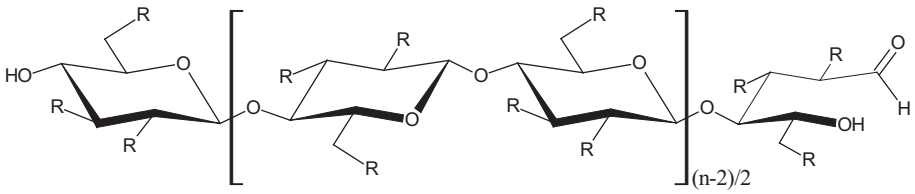

Cellulose(R = OH, Cell-$(OH)_3$)

$$\text{Cell-(OH)}_3 \xrightarrow[\text{ClCH}_2\text{COOH}]{\text{NaOH}} \text{Cell-(OH)}_{3-x}(\text{ONa})_{x-n}(\text{OCH}_2\text{COO}^-\text{Na}^+)_n \quad (\text{Cell-CH}_2\text{COONa})$$

$$\text{Cell-CH}_2\text{COONa (CMC-Na)} \xrightarrow{\text{HCl}} \text{Cell-CH}_2\text{COOH (CMC-H)} \xrightarrow{\text{LiOH}} \text{Cell-CH}_2\text{COOLi (CMC-Li)}$$

CMC (Cui, Wang, Shao, Lu, & Wang, 2011) was prepared by the slurry process in a solution of isopropyl alcohol in our laboratory, after alkalization, etherification, neutralization, washing on cellulose, we can get the CMC for this article, and DS is measured by the method of Gray alkali.

DS of CMC-Li and CMC-H depends on the DS of raw materials CMC-Na. The specific preparation process will be described in the next two paragraphs.

2.2.1. The preparation of CMC-H

The acid form of CMC was synthesized by treating CMC-Na with a HCl solution (c = 20%, wt%) in an ethanol/water mixture (95:5 by volume) for 2 h at 35 °C. Pure CMC-H was obtained by filtering, washing with an ethanol/water mixture (85:15 by volume) and drying (T = 105 °C) of the products.

2.2.2. The preparation of CMC-Li

CMC-Li was synthesized by treating the above-mentioned CMC-H in a solution of $LiOH{\cdot}H_2O$ (c = 7%, wt%) in an ethanol/water mixture (90:10 by volume) for 2 h at 50 °C. When the reaction was finished, acetic acid was added to adjust pH of the solution to pH = 7. Pure CMC-Li was obtained by filtering, washing with an ethanol/water mixture (85:15 by volume) and drying (T = 105 °C) of the products.

CMC-Lis with different DS were prepared by selecting the DS of CMC-Na and the amount of $LiOH{\cdot}H_2O$. Selecting CMC-Na with high DS (1.00) and using high amounts of $LiOH{\cdot}H_2O$, CMC-Li with DS

(1.00) was prepared, and CMC-Li with DS (0.62) was obtained from CMC-Na with high DS (0.62). In this paper, CMC-Lis with four different DS values were prepared, CMC-Li-1 (DS = 0.62, the viscosity of 2 wt% aqueous solution is 1460 mPa s), CMC-Li-2 (DS = 0.84, the viscosity of 2 wt% aqueous solution is 370 mPa s), CMC-Li-3 (DS = 1.00, the viscosity of 2 wt% aqueous solution is 54 mPa s), CMC-Li-4 (DS = 1.16, the viscosity of 2% aqueous solution is 36 mPa s).

2.3. Electrospinning

CMC-Lis were dissolved in a mixed solvent of water, and a small amount of PEO (c = 2%, wt%) was added, a solution obtained in the above steps. AQ was added into solvent and intermittent ultrasound concussion 10 min later, when CMC-Li was completely dissolved. Nano AQ/CMC-Li fibers were obtained by electrospinning device. Processing conditions were adjusted to a flow rate of 4 ml/h, with an applied voltage of 25 kV, with a capillary tip-to-target distance of 12 cm and a temperature of 25 °C. The AQ/CMC-Li composite fiber under the protection of inert gas was carbonized at a high temperature (280 °C) for two hours to obtain a modified AQ/CNF/Li nanocomposites, and then button 2032 lithium-ion battery was assembled for performance testing.

2.4. Characterization

Fourier transforms infrared spectroscopy (FT-IR) spectra of CMC and CMC-Li powders were recorded on a Nicolet 6700 infrared spectrometer (USA) with resolution of 2 cm^{-1} at room temperature. ^1H NMR spectra were obtained using a Germany Bruker ARX-400 instrument in 500 MHz. Morphology and structure of electrospun CMC-Li fibers were observed with a scanning electron microscope (SEM, JSM-6700F) after gold coating. Cyclic voltammetry (CV) and electrochemical impedance spectroscopy (EIS) results were obtained with Shanghai Chen Hua CHI660E electrochemical workstation (Shanghai, China).

The coin Cells (CR2032) were assembled to test electrochemical performance of the as-prepared AQ/CNFs, using 1 M $LiPF_6$ EC/DEC/DMC (1:1:1 by volume) as the electrolyte and a Li foil as the counter electrode. The cells were charged and discharged galvanostatically in the fixed potential window from 1.5 to 3.5 V on a Shenzhen Neware battery cycler (China) at 25 °C. The calculated capacity was based on the whole mass of the anode electrodes. CV was conducted in a cell at 0.5 mV s^{-1}. EIS was measured by applying an alternating potential of 5 mV over the frequency ranging from 10^{-2} to 20,000 Hz.

2.5. The preliminary investigation of the mechanism of the AQ/CNF/Li

Fig. 1 showed the distribution of CMC-Li in the AQ-based electrode. The performance of CMC-Li could be ascribed to strong hydrogen bonds resulting from the action of the —OH groups, which contributed to the formation of an efficient network. Sintering of the electrospun nanofiber not only removes the polymeric precursor backbone but also crystallizes the AQ nanoparticles. We propose the formation mechanism of electrospun AQ nanotubes in which partially crystallized individual AQ nanoparticles from the building blocks that self-assemble and inter-grow into a continuous fibrous morphology after the removal of volatile species at 280 °C for 2 h as following Fig. 1. If the weight ratio of CMC-Li in the electrospinning solution is higher than the metal ions, the fibers break into several segments of shorter nanorods (AQ/CNF/Li) due to the drastic structural changes when the CMC-Li backbone is heated. On the other hand, the higher DS of CMC-Li, the more freely moving lithium ion was provided with battery.

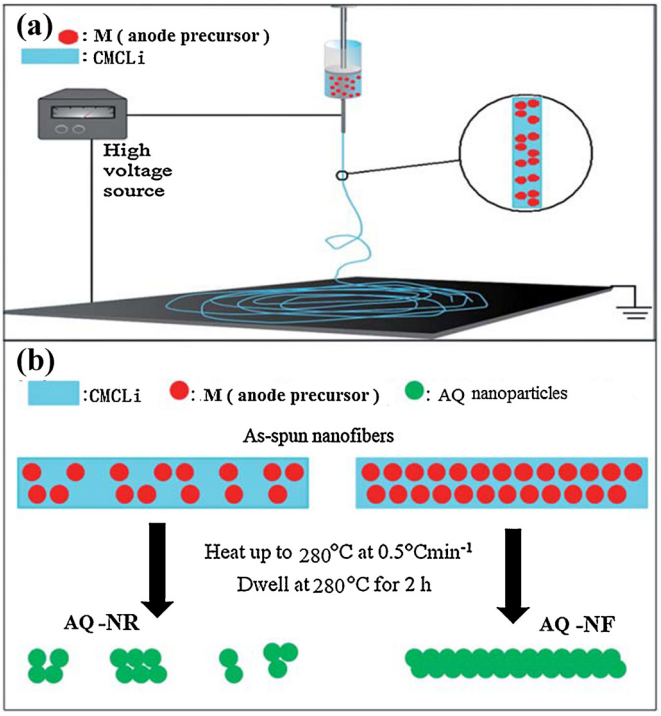

Fig. 1. The distribution of CMC-Li in the AQ electrode and a model of the mechanism. AQ/CMC-Li nanometer fiber is obtained by electrospinning, and carboniferous formation AQ/CNF/Li composite electrode material formation mechanism.

3. Results and discussion

3.1. Synthesis and characterization of CMC-Li

Fig. 2 showed the FTIR spectra of cellulose, the raw material CMC-Na, the end product CMC-Li, and the intermediate product CMC-H. All of these spectrums showed the presence of —OH stretching at 3500–3300 cm^{-1} and the CMC-H spectrum were considerably different from those of CMC-Na and CMC-Li, which indicated that the molecular structure of CMC-H changed significantly. In addition to the characteristic peaks of the common structure of ionic cellulose ether, there was more obvious difference between two kinds of carboxymethyl cellulose salt at 723 cm^{-1}, and

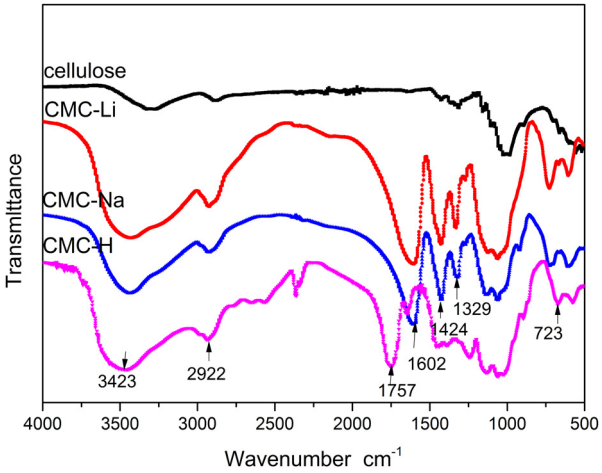

Fig. 2. FTIR spectra for Cellulose, CMC-Li, CMC-Na and CMC-H. Cellulose, CMC-Na, CMC-H and CMC-Li were successfully synthesized. By the analysis of IR spectrogram, it also confirmed the formation of the intermediate products of CMC-H, and last products CMC-Li.

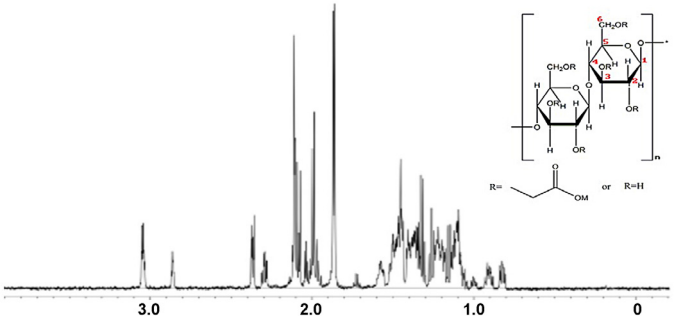

Fig. 3. The ^{1}H NMR spectrums of CMC-Li. Confirm that CMC-Li has been successfully synthesized.

it is proven that CMC-Li is successfully synthesized. IR spectra of CMC-H and CMC-Li are very different at 1757, 1602 and 1424 cm^{-1}, respectively. Because after the carboxylic acid protons are replaced by Li ions, —C=O and —C—O bonds coupled with the same carbon atom are homogenized. The size of force constant of homogenized carbon—oxygen was between double bone —C=O and single —C—O, stretching vibration of two homogenized carbon—oxygen was strong coupled, and there are two absorption bands at 1602 and 1424 cm^{-1},which confirmed the formation of CMC-H. In addition, CMC-H is insoluble in water, and after calcination of CMC-H at 700 °C for 30 min in the air, there is no residue. However, residual metallic oxides were yielded after calcination of CMC-Li and the CMC-Na. As an important intermediate product from CMC-Na to CMC-Li, CMC-H can help to judge whether the resulting product is cellulose, CMC-Na, CMC-H or CMC-Li.

The CMC-Li powder was characterized by ^{1}H NMR (Fig. 3). The different carbons of CMC-Li have been identified with numbers in Fig. 3. The ^{1}H NMR spectrum shows peaks at δ 0.7–1.6 (H from the glucose ring), δ 1.6–2.2 (H from —CH_2COO— that is attached to C3, C2-α, C2-β, and C6 from the low-field to high-field, respectively), and δ 2.2–3.1 (H from C1). The ^{1}H NMR spectrum illustrated that the molecular structure of cellulose had not been destroyed during the preparation process of CMC-Li. All of the above characterizations confirm that CMC-Li has been successfully synthesized.

3.2. SEM photos of composite fibers

Fig. 4 showed four SEM photographs before and after carbonation of AQ/CMC-Li nano-composite material. It can be seen that AQ particles were equably dispersed throughout the fiber matrix after carbonization, and then formed compound coating material of AQ/CNF/Li. Uniform distribution of AQ/CNF/Li composite material was ascribed to the fact that the particle in the spinning solution was continuing to keep down by fiber template. This provided a good solution to the problem of poor conductivity and the decline of battery performance, which was because of the nonuniform distribution of graphite in the lithium-ion battery.

3.3. The curves analysis of CV with different materials

From Fig. 5, the positions of the oxidation reduction peak of the different electrodes are distinctive. The difference in voltage between the two oxidation reduction peaks of AQ electrode coated with CMC-Li by electrospinning should be less than that of unmodified AQ. The CV curves of modified AQ electrodes are sharper than those of unmodified AQ. The distance between the discharge and charge curves of AQ/CNF/Li is smaller than that of AQ, which shows that the polarization of the former is weaker than the latter, and the difference of AQ/CNF/Li-4 and AQ electrode materials are 0.42 and 0.66 V, respectively. This may be because the AQ/CNF/Li particles were coated with the increase content of freely moving lithium ion, and unmodified AQ hindered the diffusion for lithium in the charge and discharge process of a cell.

The active material was coated with CNF/Li to form an effective ionic-conductivity layer, which provided a diffusion pathway for Li^+ to reach the active particle surface, and it enhanced the activity of electrochemical reactions. CMC-Li with the high DS was superior to that with the low DS, and the lowest redox peak of the difference is 0.42 V, the AQ/CNF/Li-4 electrode material polarization is weaker.

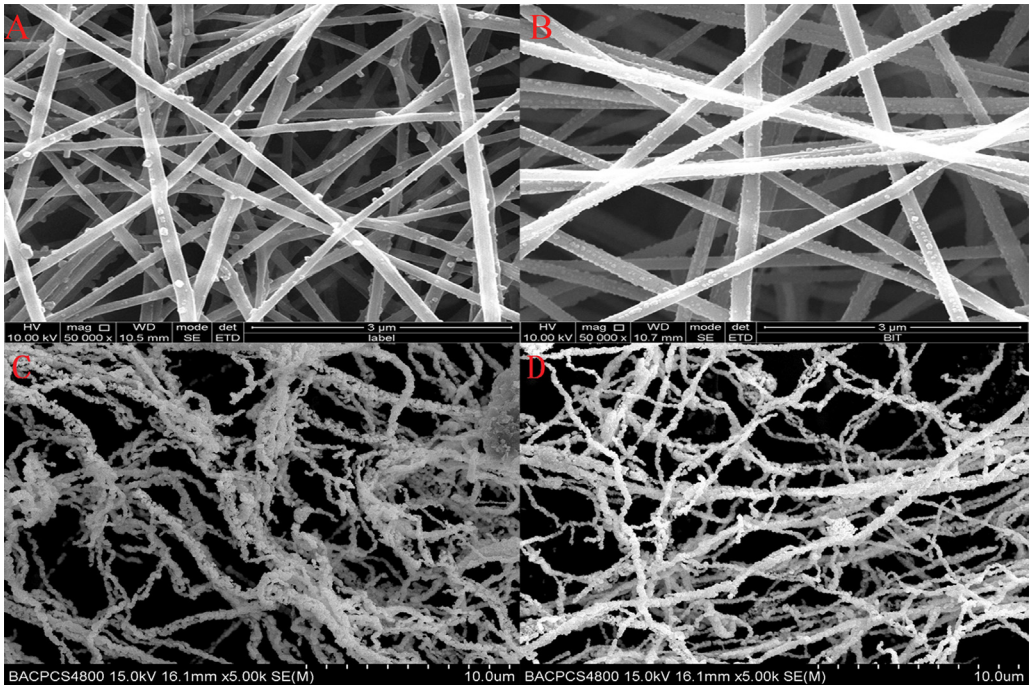

Fig. 4. SEM photos of AQ/CMC-Li composite fibers before and after modified. (A and B) before; (C and D) after. Preparation AQ/CMC-Li nanometer composite fiber, and high-temperature carbonization modified AQ/CNF/Li coated nanocomposites.

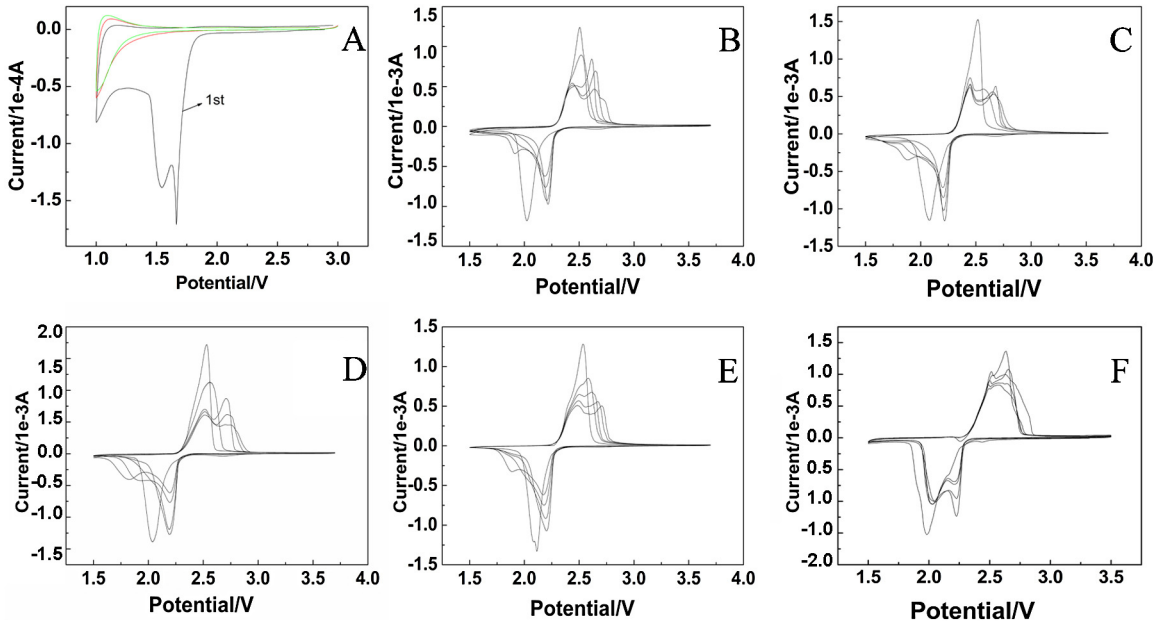

Fig. 5. The CV curves for different electrode materials. The difference of voltage to an oxidation reduction peak of electrode materials, it was seen that the irreversible reduction reaction peaks appeared between 1.5 and 1.7 V, and the AQ/CNF/Li-4 electrode material polarization is weaker.

From Fig. 5A, it was seen that the irreversible reduction reaction peaks appeared between 1.5 and 1.7 V, it shows that the cathode lithium was reacted with the $-CH_2COOH$ and $-OH$ groups of CMC-Li to form the $-CH_2COOLi$ and $-OLi$, respectively, which reduced the initial coulomb efficiency.

3.4. The curve analysis of charge and discharge with different materials

Fig. 6 showed that the first discharge specific capacity of the AQ/CNF/Li electrode was higher than that of an AQ electrode at a current density of 0.2 mA cm^{-2}. These results indicated a taller utilization ratio and electrode cycle performance of modified AQ with CMC-Li. Thus, the first discharge capacity of the AQ/CNF/Li electrode was higher than that of AQ electrode. The increase of content on $-CH_2COOLi$ equates to improve the DS of CMC-Li. And the electrode layer formed at the surface will be more stable. In addition, the increase of CNF also favored the transport of Li^+. After the same cycle, the specific capacity of AQ/CNF/Li electrode was higher than that of AQ, and AQ/CNF/Li-4 has higher capacity than other electrode materials because of its higher DS.

3.5. The curve analysis of the cycle life with different materials

It was found that the specific capacity decays of AQ and AQ/CNF/Li electrode was severe in the previous cycles from Fig. 7. However, capacity decay of AQ/CNF/Li electrode became slower after 10 cycles, and the capacity decay of AQ was faster than that

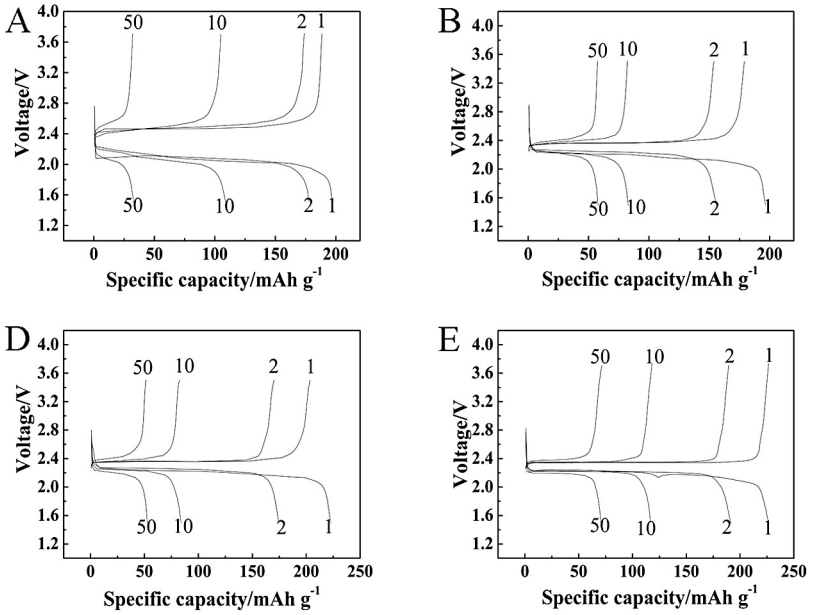

F

Modified materials	Capacity(1st) (mAh·g^{-1})	Capacity(50th) (mAh·g^{-1})
Unmodified(A)	197	33
AQ/CNF/Li-1 (B)	198	58
AQ/CNF/Li-2 (C)	214	62
AQ/CNF/Li-3 (D)	223	53
AQ/CNF/Li-4 (E)	226.4	71

Fig. 6. The charge–discharge curve of different electrode materials (2C). These results indicated a higher utilization ratio of AQ and electrode cycle performance with CMC-Li modified. AQ/CNF/Li-4 has higher capacity than other electrode materials, because it has higher DS.

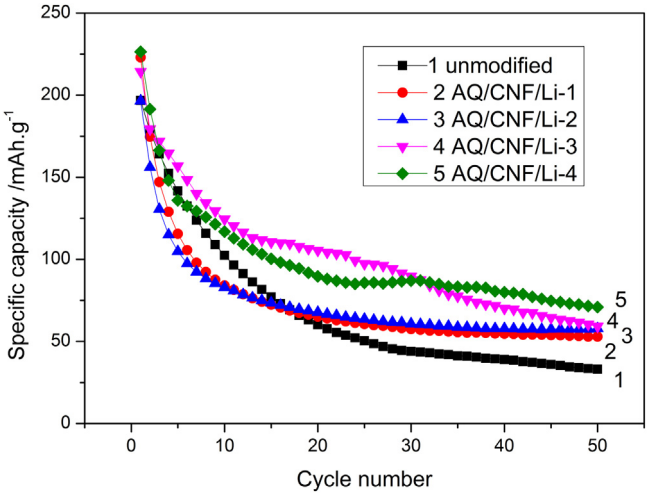

Fig. 7. The cycle life curves the AQ electrode with different modified materials. The modification way had an important effect on the cycling stability. With CMC-Li modified AQ electrode material showed improved performance by electrospinning.

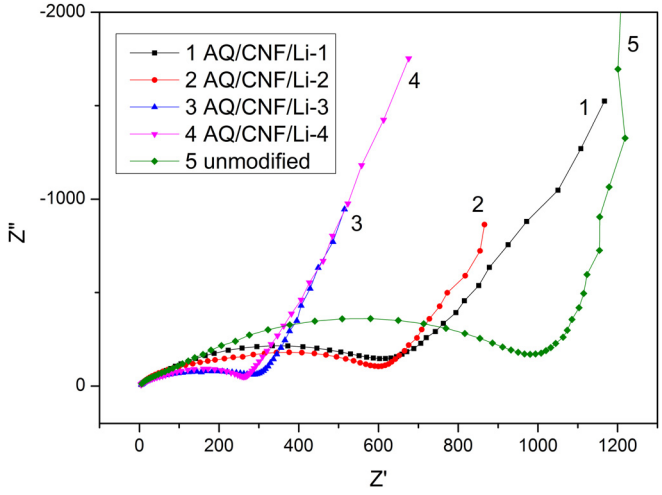

Fig. 8. Impedance responses of electrodes with different CMC-Lis. Compared with AQ, the charge-transfer resistance of a cell with AQ/CNF/Li electrode was much lower. The charge-transfer resistance of the cell by CMC-Li with high DS was obviously lower than that with low DS.

of AQ/CNF/Li. After 50 cycles, the specific capacity of the AQ electrode was maintained at 33 mAh g^{-1}, while the specific capacity of the AQ/CNF/Li-4 electrode was maintained at 71 mAh g^{-1}, and specific capacity of other modified electrode materials was much higher than that of the unmodified AQ electrode. These results confirmed that the modification way had an important effect on the cycling stability. Modified AQ electrode material with CMC-Li showed improved performance by electrospinning, and the cycle stabilities of various CMC-Li were different.

After 50 cycles, the discharge capacity of AQ/CNF/Li-3 with high DS was still higher than that of AQ/CNF/Li-1 with low DS. After 10 cycles, the curve of CMC-Li-1 was more stable, the curve of CMC-Li-3 faded rapidly, and it was not so stable. It may be because CMC-Li was synthesized by the same raw material of M100 purified cotton, the higher the DS of CMC-Li-3, the severer the degradation of cellulose molecular chain in the reaction process. So molecular weight was lower, the corresponding viscosity was smaller. Once the viscosity decreased, and it could affect the stability of the whole structure of the electrode, so it would affect electrochemical stability of the electrode in the circulation process.

3.6. The analysis of EIS with different materials

Fig. 8 showed the electrochemical impedance spectroscopy of electrode materials in the open state. Diameter size of the high-frequency semicircle reflected the size of the charge transfer resistance of a cell. Obviously, the diameters of the semicircles in the high-frequency electrodes with AQ electrode material were bigger than those for the electrodes with AQ/CNF/Li material. Compared with AQ, the charge-transfer resistance of a cell with AQ/CNF/Li electrode was much lower. These results indicated that the interfacial properties between AQ electrode and electrolyte were improved by using CNF/Li to increase the electrochemical reaction and dynamic performance. CNF/Li had played a positive role in the charge transfer process, which once again confirmed that the discharge approach of reaction between Lithium-ions on the molecular chain of CMC-Li itself adjacent to the active center and active substances in mechanism research provided a new transfer pathway for lithium-ion. For CMC-Li with different DS, the polar group numbers carried by unit mass of CMC-Li with high DS were more than those carried by CMC-Li with low DS. The repellency of CMC-Li with high DS was better, and the AQ/CNF/Li layer formed on the active grain surface was more stable. The charge-transfer resistance of the cell using CMC-Li with high DS was obviously lower than that with low DS.

4. Conclusions

Ionic cellulose derivative CMC-Li was successfully synthesized, and nanometer CMC-Li, AQ/CMC-Li, AQ/CNF/Li fiber materials were fortunately obtained by the method of electrospinning for the first time. The specific capacity, cycle performance and the decay of the same cycles of battery with AQ/CNF/Li modified electrode was better than those of unmodified AQ electrode. The electrochemical performance of modified active electrode materials by CMC-Li nanometer with the high DS was better than that with the low DS. That is, the higher the DS of CMC-Li, the better the battery electrochemical performance.

Acknowledgements

Financial support from the National Science-technology support plan projects (2011BAD23B04), special programs of graduate students' scientific and technological innovation activities of Beijing Institute of Technology (3090012241302) and Youth Science and Technology Innovation Projects of North Chemical Industry Co., Ltd. (QKCZ-BIT-04).

References

Abouimrane, A., Odom, S. A., Tavassol, H., Schulmerich, M. V., Wu, H., Bhargava, R., et al. (2013). 3-Hexylthiophene as a stabilizing additive for high voltage cathodes in lithium-ion batteries. *Journal of the Electrochemical Society*, *160*(2), A268–A271.

Canejo, J. P., & Godinho, M. H. (2013). Cellulose perversions. *Materials*, *6*(4), 1377–1390.

Chang, C., & Zhang, L. (2011). Cellulose-based hydrogels: Present status and application prospects. *Carbohydrate Polymers*, *84*(1), 40–53.

Chaudhari, S., Sharma, Y., Archana, P. S., Jose, R., Ramakrishna, S., Mhaisalkar, S., et al. (2013). Electrospun polyaniline nanofibers web electrodes for supercapacitors. *Journal of Applied Polymer Science*, *129*(4), 1660–1668.

Cui, M., Wang, F.-J., Shao, Z.-Q., Lu, F.-S., & Wang, W.-J. (2011). Influence of DS of CMC on morphology and performance of magnetic microcapsules. *Cellulose*, *18*(5), 1265–1271.

Gao, K., Shao, Z., Li, J., Wang, X., Peng, X., Wang, W., et al. (2013). Cellulose nanofiber–graphene all solid-state flexible supercapacitors. *Journal of Materials Chemistry A*, *1*(1), 63–67.

Guerfi, A., Kaneko, M., Petitclerc, M., Mori, M., & Zaghib, K. (2007). $LiFePO_4$ water-soluble binder electrode for Li-ion batteries. *Journal of Power Sources*, *163*(2), 1047–1052.

Hwang, T. H., Lee, Y. M., Kong, B.-S., Seo, J.-S., & Choi, J. W. (2012). Electrospun core–shell fibers for robust silicon nanoparticle-based lithium ion battery anodes. *Nano Letters*, *12*(2), 802–807.

Jian, Z., Zhao, L., Pan, H., Hu, Y. S., Li, H., Chen, W., et al. (2012). Carbon coated $Na_3V_2(PO_4)_3$ as novel electrode material for sodium ion batteries. *Electrochemistry Communications*, *14*(1), 86–89.

Karabulut, E., Pettersson, T., Ankerfors, M., & Wagberg, L. (2012). Adhesive layer-by-layer films of carboxymethylated cellulose nanofibril dopamine covalent bioconjugates inspired by marine mussel threads. *Acs Nano*, *6*(6), 4731–4739.

Kong, J., Yee, W. A., Wei, Y., Yang, L., Ang, J. M., Phua, S. L., et al. (2013). Silicon nanoparticles encapsulated in hollow graphitized carbon nanofibers for lithium ion battery anodes. *Nanoscale*, *5*(7), 2967–2973.

Kraytsberg, A., & Ein-Eli, Y. (2012). Higher, stronger, better... A review of 5 volt cathode materials for advanced lithium-ion batteries. *Advanced Energy Materials*, *2*(8), 922–939.

Lalia, B. S., Guillen-Burrieza, E., Arafat, H. A., & Hashaikeh, R. (2013). Fabrication and characterization of polyvinylidenefluoride-co-hexafluoropropylene (PVDF-HFP) electrospun membranes for direct contact membrane distillation. *Journal of Membrane Science*, *428*, 104–115.

Lee, S. W., Choi, S. W., Jo, S. M., Chin, B. D., Kim, D. Y., & Lee, K. Y. (2006). Electrochemical properties and cycle performance of electrospun poly(vinylidene fluoride)-based fibrous membrane electrolytes for Li-ion polymer battery. *Journal of Power Sources*, *163*(1), 41–46.

Liu, L., Fan, Q., Sun, C., Gu, X., Li, H., Gao, F., et al. (2013). Synthesis of sandwich-like TiO_2@C composite hollow spheres with high rate capability and stability for lithium-ion batteries. *Journal of Power Sources*, *221*, 141–148.

Luo, Y., Wang, S., Shen, M., Qi, R., Fang, Y., Guo, R., et al. (2013). Carbon nanotube-incorporated multilayered cellulose acetate nanofibers for tissue engineering applications. *Carbohydrate Polymers*, *91*(1), 419–427.

Ma, G., Shao, Z. Q., Wang, W. J., Wang, F. J., Tan, L. L., & Liao, B. (2010). Electrospinning of hydroxypropyl methylcellulose trimellitate solutions. *Science China-Chemistry*, *53*(1), 190–195.

Ongun, M. Z., Ertekin, K., Hizliates, C. G., Oter, O., Ergun, Y., & Celik, E. (2013). Determination of Hg(II) at sub-nanomolar levels: A comparative study with nanofibrous materials and continuous thin films. *Sensors and Actuators B*, *181*, 244–250.

Oyama, N., Pope, J. M., & Sotomura, T. (1997). Effects of adding copper(II) salt to organosulfur cathodes for rechargeable lithium batteries. *Journal of the Electrochemical Society*, *144*(4), L47–L51.

Qiu, L., Shao, Z., Yang, M., Wang, W., Wang, F., Xie, L., et al. (2013). Electrospun carboxymethyl cellulose acetate butyrate (CMCAB) nanofiber for high rate lithium-ion battery. *Carbohydrate Polymers*, *96*(1), 240–245.

Rodriguez, K., Renneckar, S., & Gatenholm, P. (2011). Biomimetic calcium phosphate crystal mineralization on electrospun cellulose-based scaffolds. *ACS Applied Materials & Interfaces*, *3*(3), 681–689.

Rousselot, S., Gauthier, M., Mazouzi, D., Lestriez, B., Guyomard, D., & Roue, L. (2012). Synthesis of boron-doped Si particles by ball milling and application in Li-ion batteries. *Journal of Power Sources*, *202*, 262–268.

Saji, V. S., Kim, Y. S., Kim, T. H., Cho, J., & Song, H. K. (2011). One-dimensional (1D) nanostructured and nanocomposited LiFePO(4): its perspective advantages for cathode materials of lithium ion batteries. *Physical Chemistry Chemical Physics*, *13*(43), 19226–19237.

Teh, P. F., Sharma, Y., Pramana, S. S., & Srinivasan, M. (2011). Nanoweb anodes composed of one-dimensional, high aspect ratio, size tunable electrospun ZnFe(2)O(4) nanofibers for lithium ion batteries. *Journal of Materials Chemistry*, *21*(38), 14999–15008.

Vulic, K., & Shoichet, M. S. (2012). Tunable growth factor delivery from injectable hydrogels for tissue engineering. *Journal of the American Chemical Society*, *134*(2), 882–885.

Wang, J., Yu, Y., Gu, L., Wang, C., Tang, K., & Maier, J. (2013). Highly reversible lithium storage in Si (core)-hollow carbon nanofibers (sheath) nanocomposites. *Nanoscale*, *5*(7), 2647–2650.

Wang, W., Xu, W., Cosimbescu, L., Choi, D., Li, L., & Yang, Z. (2012). Anthraquinone with tailored structure for a nonaqueous metal-organic redox flow battery. *Chemical Communications*, *48*(53), 6669–6671.

Wu, Y., Zhu, P., Zhao, X., Reddy, M. V., Peng, S., Chowdari, B. V. R., et al. (2013). Highly improved rechargeable stability for lithium/silver vanadium oxide battery induced via electrospinning technique. *Journal of Materials Chemistry A*, *1*(3), 852–859.

Xie, L., Shao, Z., Wang, W., & Wang, F. (2011). Preparation of AlNPs/NC composite nanofibers by electrospinning. *Integrated Ferroelectrics*, *127*, 184–192.

Xie, L., Zhao, L., Wan, J.-l., Shao, Z.-q., Wang, F.-j., & Lv, S.-y. (2012). The electrochemical performance of carboxymethyl cellulose lithium as a binding material for anthraquinone cathodes in lithium batteries. *Journal of the Electrochemical Society*, *159*(4), A499–A505.

Yu, D.-G., Yu, J.-H., Chen, L., Williams, G. R., & Wang, X. (2012). Modified coaxial electrospinning for the preparation of high-quality ketoprofen-loaded cellulose acetate nanofibers. *Carbohydrate Polymers*, *90*(2), 1016–1023.

Yu, D. G., Wang, X., Li, X. Y., Chian, W., Li, Y., & Liao, Y. Z. (2013). Electrospun biphasic drug release polyvinylpyrrolidone/ethyl cellulose core/sheath nanofibers. *Acta Biomaterialia*, *9*(3), 5665–5672.

Zhang, X., Lin, Z., Chen, B., Sharma, S., Wong, C.-p., Zhang, W., et al. (2013). Solid-state, flexible, high strength paper-based supercapacitors. *Journal of Materials Chemistry A*, *1*(19), 5835–5839.

Zhao, H., Lu, B., Xu, J., Xie, E., Wang, T., & Xu, Z. (2013). Electrospinning-thermal treatment synthesis: a general strategy to decorate highly porous nanotubes on both internal and external side-walls with metal oxide/noble metal nanoparticles. *Nanoscale*, *5*(7), 2835–2839.

Zhou, X., Yin, Y.-X., Cao, A.-M., Wan, L.-J., & Guo, Y.-G. (2012). Efficient 3D conducting networks built by graphene sheets and carbon nanoparticles for high-performance silicon anode. *ACS Applied Materials & Interfaces*, *4*(5), 2824–2828.